

## Globular structure of human ovulatory cervical mucus

Roberto Brunelli,<sup>\*,1</sup> Massimiliano Papi,<sup>†,1</sup> Giuseppe Arcovito,<sup>†</sup> Adriano Bompiani,<sup>§</sup> Massimo Castagnola,<sup>‡,§,||</sup> Tiziana Parasassi,<sup>¶</sup> Beatrice Sampaolese,<sup>||</sup> Federica Vincenzoni,<sup>§</sup> and Marco De Spirito<sup>†,2</sup>

<sup>\*</sup>Dipartimento di Scienze Ginecologiche, Perinatologia e Puericultura, Università di Roma *La Sapienza*, Italy; <sup>†</sup>Istituto di Fisica; <sup>§</sup>Istituto Scientifico Internazionale “Paolo VI,” Rome, Italy; and <sup>‡</sup>Istituto di Biochimica e Biochimica clinica, Facoltà di Medicina e Chirurgia, Università Cattolica del Sacro Cuore, Rome, Italy; and <sup>||</sup>Istituto per la Chimica del Riconsimento Molecolare and <sup>¶</sup>Istituto di Neurobiologia e Medicina Molecolare, CNR, Rome, Italy

**ABSTRACT** Human cervical mucus is a heterogeneous mixture of mucin glycoproteins whose relative concentration changes during the ovulatory phases, thereby producing different mucus aggregation structures that can periodically permit the transit of spermatozoa for fertilization. In preovulatory phase, mucus is arranged in compact fiber-like structures where sperm transit is hindered. Previously, through observations made of fixed and dehydrated samples, a permissive structure in the ovulatory phase was attributed to the larger diameters of pores in the mucus network. Instead, by means of atomic force microscopy, we can show, for the first time, that unfixed ovulatory mucus is composed by floating globules of mucin aggregates. This finding sheds new light on the mechanism that governs spermatozoa transit toward the uterine cavity. In addition, we demonstrate that the switch from globular ovulatory to fibrous preovulatory mucus largely depends on a pH-driven mechanism. Analysis of mucin 5B primary sequence, the main mucin in ovulatory mucus, highlights pH-sensitive domains that are associated to flexible regions prone to drive aggregation. We suggest an involvement of these domains in the fiber-to-globule switch in cervical mucus.—Brunelli, R., Papi, M., Arcovito, G., Bompiani, A., Castagnola, M., Parasassi, T., Sampaolese, B., Vincenzoni, F., De Spirito, M. Globular structure of human ovulatory cervical mucus. *FASEB J.* 21, 000–000 (2007)

*Key Words:* atomic force microscopy • hydrophobicity • MUC5B • recurrence analysis.

THE CERVICAL CANAL of the uterus is covered by a thin layer of mucus, a highly hydrated viscoelastic gel composed of a group of extraordinarily long, glycosylated, highly hydrated proteins known as mucins (1) whose physical, chemical, rheological, and hydrodynamic properties change dramatically during the ovulatory period (1). During a normal menstrual cycle, but outside the ovulatory phase, the mucus is scant, thick, and viscous, therefore forming a physical barrier that limits the access of sperm to the genital tract. In difference, immediately before ovulation cervical mu-

cus viscosity decreases, thereby maximizing its permeability to sperm (2, 3).

It is reasonable to suppose that all these features reflect variations in the molecular and compositional properties of cervical mucins, whose relative abundance varies during the menstrual cycle. Actually, steroid hormones strongly influence mucin biosynthesis in endocervical cells, and mucin 5B (MUC5B) becomes the principal mucin present in human ovulatory cervical mucus (4, 5).

The first light microscopy studies of ovulatory cervical mucus identified a characteristic fern-like crystallization of salts and postulated that this was dependent on a peculiar structural organization of mucin molecules (6–8). A more accurate knowledge of the mucus salt crystal structure and ferning patterns was obtained by the use of scanning electron microscopy (8, 9), but no direct structural information on the mucin component of the mucus was obtained. Further investigations were carried out using polarization microscopy and conventional X-ray devices focused on anisotropic structures composed of sodium and potassium sulfates (10, 11), but again with no specific reference to mucin proteins. Nuclear magnetic resonance suggested an ultrastructure for human cervical mucus composed of a linear arrangement of mucoïd molecules grouped together in parallel bundles (12, 13). Microscopy observations on virtually salt-free mucins revealed honeycomb and filamentous mucus structures, although with large discrepancies in the determined intra- and intermolecular dimensions, in a range of two orders of magnitude (14–16). On a whole, great variations due to samples preparation and, more importantly, in artifacts due to fixation and dehydration, can well account for the differences in descriptions of mucus microstructure reported in more than 30 y of microscopic observations.

The general consensus (14–16) is that, at ovulation,

<sup>1</sup> These authors contributed equally to this work.

<sup>2</sup> Correspondence: Istituto di Fisica, Facoltà di Medicina e Chirurgia, Università Cattolica del Sacro Cuore, Largo F. Vito 1, 00168 Rome, Italy. E-mail: m.despirito@rm.unicatt.it  
doi: 10.1096/fj.07-8189com

pore size within the mesh of interconnected mucin filaments enlarges. However, factors determining the periovalutary mucus's lower viscosity, and therefore increased permeability to sperm, in comparison with other menstrual phases, are still largely unknown. To investigate some of these open questions, we developed a different, non-perturbative, approach.

Tapping mode atomic force microscopy (AFM) in an aqueous environment was recently shown to be a useful and nonperturbative technique for the study of glycoprotein structure and aggregation (17). We used tapping mode AFM to image human cervical mucus during the different phases of the menstrual cycle. In agreement with previous observations, our results show that preovulatory mucus is arranged in a dense filamentous structure. Conversely, we could show for the first time that ovulatory mucus displays rather a different organization, consisting in dispersed floating globules of aggregated mucin molecules. These ovulatory globules differ from all previously reported mucus structures and can well justify both its dramatically decreased viscosity and increased permeability to sperm.

Even in the absence of compositional change, we also demonstrated that a reversion from the globular to the compact fiber-like arrangement can easily be obtained in the ovulatory mucus by lowering the pH. In addition to a marginal role of salt and carbohydrate variations, whose relevance was previously claimed (18), this result strongly suggests a fundamental involvement of mucin primary structure. Indeed, analysis of MUC5B primary sequence highlights domains sensitive to pH variation and flexible, aggregation-prone regions.

## MATERIALS AND METHODS

### Atomic force microscopy

AFM imaging was performed using an SPMagic SX Atomic Force Microscope (Elbitech, Italy) in the tapping operation mode; samples were kept in an aqueous environment throughout the measurement procedure. This approach was aimed to minimize perturbations and artifacts due to salt crystallization following dehydration. The microscope probe consisted of an ultrasharp silicon nitride cantilever of nominal force constant  $k = 40$  N/m with a tip radius of less than 10 nm (NSC16 MikroMash). Image analysis was performed using a WSxM software (Nanotec Electronica S.L., Spain). Samples were laid down on freshly cleaved mica. All images were flattened with a zero- or first-order polynomial fit, and for each image an appropriate threshold value of the contrast was set to discriminate between objects and background.

### Determination of menstrual phase and preparation of human cervical mucus for AFM

The ovulatory phase was established in healthy volunteers by a fast quantitation of LH urinary peak using the Clearplan™ kit (Unipath, Bedford, UK). Twenty-four hours after a positive test, the ovulatory mucus sample was collected by aspiration from the cervical canal with a catheter for intrauterine insemination (Gynetics Medical Products, Achel, Belgium). 17- $\beta$ -estradiol was also determined in plasma and found

compatible with the predicted values of the ovulatory phase. Acidification was performed by using TRIS buffer at pH 6.0. Preovulatory mucus was collected after a negative test and on the 7<sup>th</sup> day.

### Recurrence analysis

An available method for analyzing the physico-chemical properties (i.e., hydrophobicity) of an amino acid sequence is the recurrence analysis (RA). RA is a nonlinear time-series analysis method (19) based on the projection of the original monodimensional series into a multidimensional space constituted by subsequently lagged copies of the original sequence. For any ordered series (temporal or spatial), a recurrence is defined as a point that repeats itself. In the case of a polypeptide chain expressed by the values of a physico-chemical property (i.e., hydrophobicity) of residues, recurrences are patches of residues of predefined length having a profile similar to other patches of the same length along the numerical profile of the chain. The recurrence plot (RP), a 2D plot of the recurrences of the protein primary structure, allows for an easy visualization of the results of this analysis. We coded the MUC5B sequence, obtained from the Swiss-prot database, using the Miyazawa-Jernigan hydrophobicity scale (MJ). MJ corresponds to the first eigenvalue of the contact energy matrix and allows one to obtain the largest separation in distance space for obtained patterns, as compared to a random assortment of amino acids (20). This coded sequence was analyzed by RA, and the results were plotted so as to visualize the hydrophobicity autocorrelation along the sequence. A high concentration of hydrophobicity recurrences aligned parallel to the main diagonal of the RP is indicated as determinism and is correlated with aggregation/folding propensity (20, 21).

The isoelectric point was determined using ProtParam software (22).

## RESULTS

In **Fig. 1A** we report a representative tapping mode AFM image of human preovulatory mucus obtained from a sample taken on the 7<sup>th</sup> day of the menstrual cycle. The hydrogel appears very homogenous, with a net of interconnected fibers. The average mesh size is of  $500 \pm 250$  nm, and the fibers' diameters range between 10 and 500 nm. It is noteworthy that, this structure is consistent with the reported polymeric linear concatenation and lateral aggregation of gastric mucin (17, 23–26).

This intricate fibrous hydrogel structure of the preovulatory mucus significantly differs from what was seen in the ovulatory mucus, where several compact spherical structures are visible (**Fig. 1B**). Their average size of  $600 \pm 200$  nm is compatible with the aggregation of several mucin molecules. Globules occasionally bridge together, thus creating a short pearl necklace structure, which can be seen enlarged in (**C**). These dispersed globules have never been revealed before in ovulatory mucus. Simply by dehydrating samples, we reproduced the fern-like structure previously reported for ovulatory mucus (8) (not shown). We therefore concluded that the globules imaged in hydrated and unfixed samples more realistically represent mucus structure.

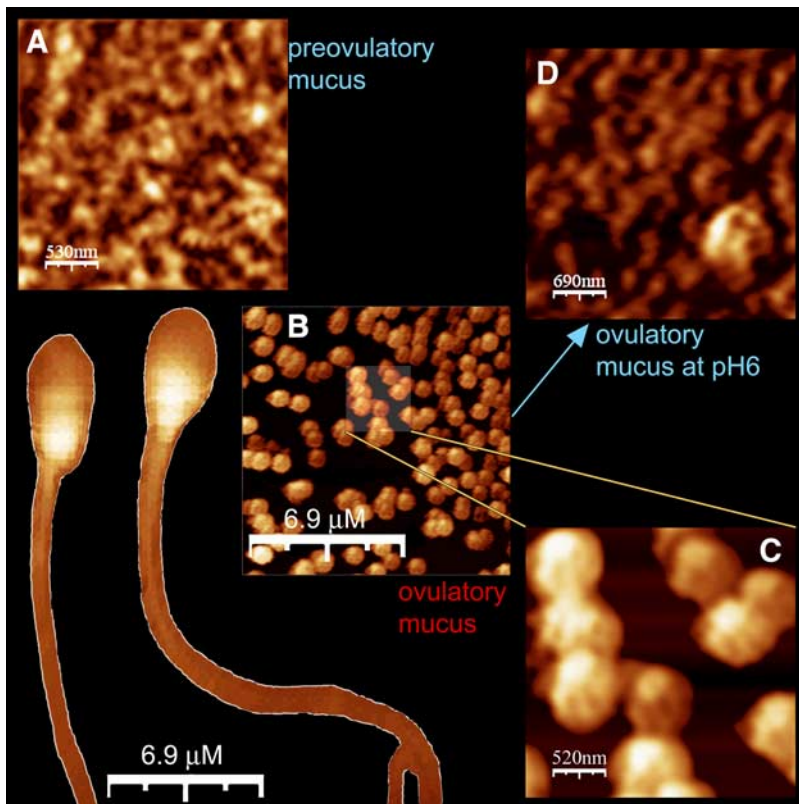


**Figure 1.** Different structures of human cervical mucus during the menstrual cycle. Tapping mode AFM images of: preovulatory mucus (A), ovulatory mucus (B) with a detail enlarged (C); ovulatory mucus at pH 6 (D). Two spermatozoa are also imaged (left side of the image) at the same magnification as the ovulatory mucus (B) to facilitate comparison.

In the background of Fig. 1 we show two spermatozoa, captured in a sample and imaged at the same magnification as the ovulatory mucus, to give a direct representation of how easy their transit might be among the dispersed and floating mucus globules.

The mucus's permeability to sperm peaks at midcycle, when cervical pH is relatively high, while it decreases outside the ovulatory period, when pH is as low as 6.2 (27). We therefore explored the influence of pH on the structure of these newly evidenced mucin globules by lowering to 6 the pH of the ovulatory mucus sample. The AFM images obtained show a dramatic modification, exemplified in (D), with the disappearance of globules, substituted by an entangled network that closely resembles the preovulatory mucus imaged in (A).

We then focused our attention on the study of the primary structure of MUC5B in order to find out whether it possesses intrinsic characteristics that may make it responsive to pH variation and prone to structural change. Our analysis was performed in terms of hydrophobicity, determinism, and isoelectric point.

The primary structure of MUC5B was expressed through hydrophobicity values, as coded by means of the Miyazawa-Jernigan hydrophobicity scale, and the results are plotted in panel B of Fig. 2. The plot allowed for easy identification of three well-resolved regions: a central region with lower hydrophobicity values, averaged to 4.9, between residues 1100 and 3700, and two outer regions of higher hydrophobicity, averaged to 5.5.

In close correspondence with these different hydrophobicity sections, the study of MUC5B sequence space by means of recurrence analysis also revealed three well-resolved regions (Fig. 2C). In a recurrence plot,

dots aligned along the main diagonal indicate highly deterministic regions of the primary sequence, corresponding to several repetitive amino acid sequences. Highly deterministic regions are implicated in aggregation, folding, and flexibility (20, 21). Indeed, in MUC5B a highly deterministic region occurred between residues 1100 and 3700 (Fig. 2C), overlapping the central lower hydrophobicity region (Fig. 2B). Conversely, the two outer regions with higher hydrophobicity were characterized by a negligible determinism. A more detailed examination of the central region of MUC5B showed that it is regularly spaced by conspicuous hydrophobicity peaks (Fig. 2B) exactly matching low determinism sequences (Fig. 2C). Following a previously reported characterization (28), these peaks can be identified as the cysteine rich domains.

Given the influence of pH on mucus structure, as demonstrated above, we also examined the isoelectric point of residues in the primary sequence of MUC5B. A remarkably higher average isoelectric point of 8.1 characterized the central region with respect to the values of 5.3 and 5.6 calculated in the left and right outer regions, respectively (PI line in Fig. 2).

On the whole, the central region of MUC5B is characterized by low hydrophobicity, high determinism, high isoelectric point, and regularly spaced highly hydrophobic cysteine rich domains.

## DISCUSSION

In difference to the view that changes in structure and viscosity of human cervical mucus have to be attributed

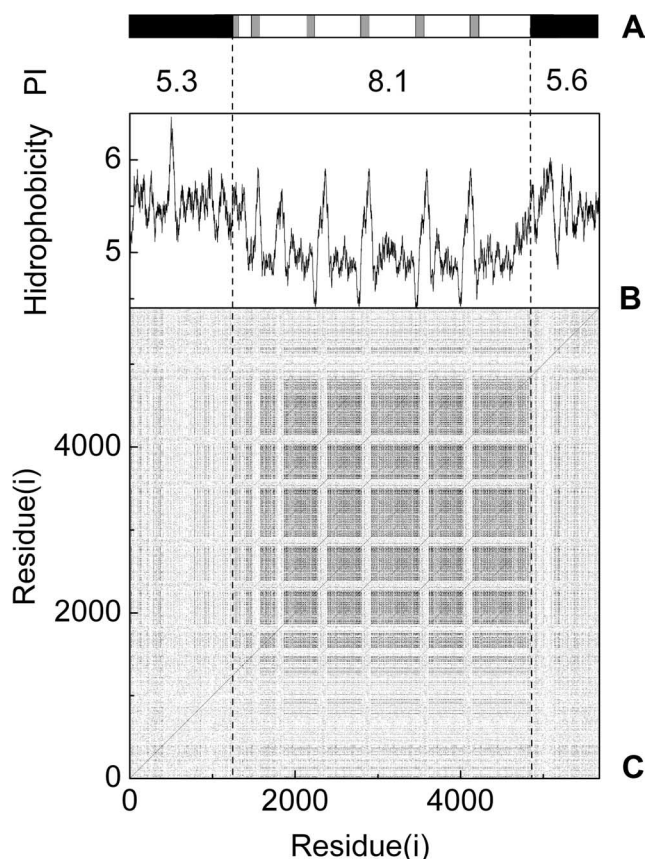


**Figure 2.** Properties of the MUC5B primary structure. *A*) Sketched domains of MUC5B: outer domains in black, central domain in white and cysteine rich domains in light gray. *PI*. The isoelectric point is reported for each region. *B*) Hydrophobicity values of MUC5B as coded by means of the Miyazawa-Jernigan hydrophobicity scale. *C*) Recurrence analysis of MUC5B showing highly deterministic regions in dark gray.

to the different size of pores within the mesh of interconnected filaments (14–16), we provide here the first evidence that ovulatory mucus possesses a structure quite different from that previously imaged, consisting, indeed, of floating globules of mucin aggregates. This advance in knowledge provides an immediate explanation for easier spermatozoa transit toward the uterine cavity during ovulation and was achieved by an imaging technique that does not require sample dehydration and fixation. In this context it would be of interest to investigate on the different morphological types of cervical mucus that have been described, including specific secretions from cervical canal crypts (8).

The globular structure can be transformed to a fibrous net simply by sample acidification. This finding minimizes the relevance of compositional changes, both in terms of carbohydrates and salts (29), and highlights a simple regulatory mechanism for both the mucus's structure and sperm transit. As a peripheral observation, these results fit well with the relative alkalinity of ovulatory mucus and the old clinical notion that mucus alkalization helps in improving permeability to sperm (6)

The dependence on the pH of mucus structure prompted us to analyze the primary sequence of the main mucin present during ovulation: the MUC5B. Our results allowed for the identification of a central region characterized by low hydrophobicity, high determinism—therefore showing a high propensity to aggregation, folding and flexibility (20, 21)—and higher isoelectric point, well resolved from the two outer regions displaying opposite properties. Cysteine-rich domains present in this central region can stabilize aggregates by forming intermolecular disulfur bondings. Indeed, we observed that the addition of 5% dithiothreitol destabilized the globular structure of ovulatory mucus (not shown).

Due to these structural features we can reasonably hypothesize that in the alkaline environment of the ovulatory mucus the globular aggregates originate from the following properties of the central region: i) formation of intermolecular disulfur bondings; ii) flexibility; and iii) absence of an electrostatic screening.

To induce a globular-to-fibrous switch in ovulatory mucus, we used a pH value compatible with the isoelectric point of the two outer domains and close to the characteristic pH value outside the ovulatory period, of ~6 (27). Interestingly, in gastric mucin fibrous structures have been obtained at low pH and were interpreted as the result of intermolecular hydrophobic interactions (26). Similarly, in acidic environments the two outer hydrophobic domains of MUC5B, close to their isoelectric point, could represent the driving force for an end-to-end intermolecular hydrophobic interaction that forms the fibrous net. Concurrently, the electrostatic repulsion in the central region will hinder lateral intermolecular aggregation.

In conclusion, we have disclosed new and striking morphological features of human cervical ovulatory mucus, with a globular structure, which are definitely different from the compact and fibrous mesh that represents the signature of preovulatory mucus. This evidence constitutes a novel morphological counterpart to the old notion that ovulatory mucus displays maximum permeability to sperm and minimum viscosity. This globular structure depends on MUC5B primary structure.

Given the similar pH sensitivity of gastric mucin in its switch between different structural arrangements (26), we anticipate that a primary sequence analysis method similar to that reported here could help in modeling pH role in the modulation of other mucins' structural properties. FJ

Our thanks go to Graziella Costa for her skilful technical assistance. This research was partially supported by the Università Cattolica S. Cuore, Rome, Italy, and by the Italian Ministry of University and Research (COFIN 2004).

## REFERENCES

1. Lagow, E., DeSouza, M. M., and Carson, D. D. (1972) Mammalian reproductive tract mucins. *Hum. Reprod. Update* **5**, 280–292

2. Moghissi, K. S. (1972) The function of the cervix in fertility. *Fertil. Steril.* **23**, 295–306
3. Wolf, D. P., Blasco, L., Khan, M. A., and Litt, M. (1978) Human cervical mucus. IV. Viscoelasticity and sperm penetrability during the ovulatory menstrual cycle. *Fert. Ster.* **30**, 163–169
4. Gipson, I. K., Moccia, R., Spurr-Michaud, S., Argueso, P., Gargiulo, A. R., Hill, J.A. 3rd, Offner, G. D., and Keutmann, H. T. (2001) The amount of MUC5B mucin in cervical mucus peaks at midcycle. *J. Clin. Endocrinol. Metab.* **86**, 594–600
5. Gipson, I.K., Spurr-Michaud, S., Moccia, R., Zhan Q., Toribara, N., Ho, S.B., Gargiulo, A. R., and Hill, J. A. 3rd (1999) MUC4 and MUC5B Transcripts are the prevalent mucin messenger ribonucleic acids of the human endocervix. *Biol. Reprod.* **60**, 58–64
6. Papanicolaou, G. N. (1946) A general survey of the vaginal smear and its use in research and diagnosis. *Am. J. Obstet. Gynecol.* **51**, 316–328
7. Rydberg, E. (1948) Observation on the crystallization of the cervical mucus. *Acta Obstet. Gynecol. Scand.* **28**, 172–187
8. Menárguez, M., Pastor, L. M., and Odeblad, E. (2003) Morphological characterization of different human cervical mucus types using light and scanning electron microscopy. *Hum. Reprod.* **18**, 1782–1789
9. Zaneveld, L. J., Tauber, P. F., Port, C., and Propping, D. (1975) Scanning electron microscopy of cervical mucus crystallization. *Obstet. Gynecol.* **46**, 419–428
10. Chretien, F. C., and Berthou, J. (1991) Anisotropic crystalline microstructures in dendritic arborizations of dried mid-cycle cervical mucus: surface morphology and crystallographic study. *Hum. Reprod.* **6**, 1192–1199
11. Chretien, F. C., and Berthou, J. (1989) A new crystallography approach to fern-like microstructures in human ovulatory cervical mucus. *Hum. Reprod.* **4**, 359–368
12. Odeblad, E. (1961) Micro NMR in high permanent magnetic fields. Theoretical and experimental investigations with an application to the secretions from single glandular unit in the human uterine cervix. *Acta Obstet. Gynecol. Scand.* **45 (Suppl. 2)**, 127–129
13. Odeblad, E. (1968) The functional structure of human cervical mucus *Acta Obstet. Gynecol. Scand.* **45**, 57–60
14. Yudin, A. I., Hanson, F. W., and Katz, D. F. (1989) Human cervical mucus and its interaction with sperm: a fine-structural view. *Biol. Reprod.* **40**, 661–671
15. Ceric, F., Silva, D., and Vigil, P. (2005) Ultrastructure of the human periovulatory cervical mucus. *J. Electron. Microsc.* **54**, 479–484
16. Chretien, F. C., Gernigon, C., David, G., and Psychoyos, A. (1973) The ultrastructure of human cervical mucus under scanning electron microscopy. *Fertil. Steril.* **24**, 746–757
17. Hong, Z., Chasan, B., Bansil, R., Turner, B. S., Bhaskar, K. R., and Afdhal, N. H. (2005) Atomic force microscopy reveals aggregation of gastric mucin at low pH. *Biomacromolecules* **6**, 3458–3466
18. Yurewicz, E. C., Matsuura, F., and Moghissi, K. S. (1982) Structure characterization of neutral oligosaccharides of human midcycle cervical mucin. *J. Biol. Chem.* **257**, 2314–2322
19. Webber, C.L. Jr., and Zbilut, J. P. (1994) Dynamical assessment of physiological systems and states using recurrence plot strategies. *J. Appl. Physiol.* **76**, 965–973
20. Zbilut, J. P., Colosimo, A., Conti, F., Colafranceschi, M., Manetti, C., Valerio, M. C., Webber, C.L. Jr., and Giuliani, A. (2003) Protein aggregation/folding: the role of deterministic singularities of sequence hydrophobicity as determined by nonlinear signal analysis of acylphosphatase and A $\beta$ (1–40). *Biophys. J.* **85**, 3544–3557
21. Giuliani, A., Benigni, R., Sirabella, P., Zbilut, J. P., and Colosimo, A. (2000) Nonlinear methods in the analysis of protein sequences: a case study in rubredoxins. *Biophys. J.* **78**, 136–148
22. Gasteiger, E., Hoogland, C., Gattiker, A., Duvaud, S., Wilkins, M.R., Appel, R.D., and Bairoch, A. (2005) Protein identification and analysis tools on the ExPASy server. In *The Proteomics Protocols Handbook* (Walker, J.M., ed) pp. 571–607, Humana Press, Totowa, NJ, USA.
23. Bhaskar, K.R., Garik, P., Turner, B.S., Bradley, J.D., Bansil, R., Stanley, H. E., and LaMont, J. T., (1992) Viscous fingering of HCl through gastric mucin. *Nature* **360**, 458–461
24. Cao, X., Bansil, R., Bhaskar, K. R., Turner, B. S., LaMont, J. T., Niu, N., and Afdhal, N. H. (1999) pH-Dependent Conformational Change of Gastric Mucin Leads to Sol-Gel Transition. *Biophys. J.* **76**, 1250–1258
25. Hong, Z., Bansil R., Waigh, T., Turner, B., Bhaskar, K.R., Afdhal, N. and Lal, J. (2002) Small angle neutron scattering (SANS) study of gastric mucin solutions. American Physical Society, Annual APS March Meeting
26. Bansil, R., Cao, X., Bhaskar, K. R., and LaMont, J. T. (1997) Dynamic light-scattering study of gelatin and aggregation of gastric mucin. *Proc. SPIE.* **2982**, 116–125
27. Eggert-Kruse, W., Kohler, A., Rohr, G., and Runnebaum, B. (1993) The pH as an important determinant of sperm-mucus interaction. *Fert. Ster.* **59**, 617–628
28. Perez-Vilar, J., and Hill, R. L. (1999) The structure and assembly of secreted mucins. *J. Biol. Chem.* **274**, 31751–31754
29. Yurewicz, E. C., Matsuura, F., and Moghissi, K. S. (1982) Structure Characterization of Neutral Oligosaccharides of Human Midcycle cervical Mucin. *J. Biol. Chem.* **257**, 2314–2322

Received for publication ???.

Accepted for publication ???.